MULTI-MATERIAL SHAPE MEMORY POLYMERS: DESIGN CONSIDERATIONS AND IMPLEMENTATION

Alexandru Sover[1][0000-0003-3408-898X], Vasile Ermolai[1][0000-0001-5967-5748]*
[1]Ansbach University of Applied Science, Ansbach, Germany
E-mail: a.sover@hs-ansbach.de

Abstract – Shape memory polymers (SMP) are material systems capable of changing shape in response to external stimuli. By integrating multiple materials in the same system, the shape SMPs' can produce multiple shape/geometrical changes proportional to the number of constituents. Multi-material Fused Filament Fabrication (FFF) introduced new development possibilities regarding SMPs. However, materials integration is limited due to the affinity of polymeric materials. This research proposes a design framework adapted for multi-material printing for low-compatibility polymers to solve some of these limitations. This way, using some design principles for FFF and multi-material printing can integrate two or more materials into the same component. In the end, the principles were used to print and test eight TPU/PLA-based SMSs.

Keywords: Shape Memory Polymer, 4D printing, Multi-material printing, Design for multi-material printing, Shape recovery

1. Introduction

Shape Memory Materials (SMM) are material structures that can modify their shape in response to an external stimulus [1-4]. By incorporating different materials, multi-material SMM can exhibit enhanced mechanical properties, improved shape recovery, and tailored responses to stimuli [4-9].

Depending on the constituting materials, the SMM can be divided into Shape Memory Alloys, SMAs (e.g., NiTi [10, 11], Cu-Al-Ni [1]), and Shape Memory Polymers, SMPs, (e.g., PLA/TPU [12, 13], PET/PA [14]) [2, 3, 9, 15, 16]. On the one hand, SMAs are characterised by higher recovery stress and strain and exert higher forces during recovery [10, 17]. On the other hand, SMPs are characterised by lightweight [1,2] and high deformability [16,18] and can incorporate multiple shape change sequences [2, 3, 7, 18]. For the SMPs, the shape recovery can be triggered by stimuli such as heat, light, moisture, pH, electrical and magnetic fields [2, 8, 15, 18, 19].

The SMPs are made from a variety of polymeric materials including but not limited by thermoplastic polyurethane (TPU) [4], polyamide (PA) [5, 8, 14], polylactic acid (PLA) [4, 20, 21], polycaprolactone (PLC) [8]. Furthermore, SMPs include other materials, such as hydrogels [19] and foams [18]. Blends of different polymeric materials [12] or the addition of fillers (e.g., particles and fibres) can also be used to modify the properties of SMPs, such as engineering a recovery mechanism, improving their thermal stability, increasing their strength and stiffness [1, 4, 18, 22].

Depending on the number of components, the SMPs can be classified as single, double, triple, or multi-material systems [2, 7, 23]. However, regardless of the number of components, the SMPs' working principle is based on the dual-state, dual-component, and partial transition mechanism [2, 4, 6-8,16, 23]. In the first case, dual-state, the permanent shape is provided by the covalent bond of the polymeric chains, while the temporary shape is maintained by the chains' rearranged entanglements [20, 21, 24]. In the second case, dual-component or multi-component (depending on the number of integrated materials), the permanent shape is maintained by a rigid polymer and the temporary by a softer one [5, 13, 14]. In the third mechanism, partial transition, polymeric materials are incorporated in a blend to obtain a similar effect to the second mechanism [12, 19, 22].

SMPs can be produced conveniently through Additive Manufacturing (AM), including but not limited by Stereolithography (SLA), Selective Laser Sintering (SLS) or material extrusion technologies such as Fused Deposition Modeling (FDM)/Fused Filament Fabrication (FFF) [8, 9, 18, 25, 26]. The SMPs 3D Printing is often called 4D printing because the shape change occurs in a time [1, 8, 15, 18]. Even if polymeric AM technologies provide high freedom in the design process of a product, the integration of multiple materials is limited to the constituents' compatibility. For this reason, certain combinations of polymers are not possible due to their lack of affinity (e.g., PA/ABS, PA/PETG [27]).

This work mainly focused on developing an SMP design framework for the multi-material FFF AM technology that integrates good and low-compatibility polymers in the same manufacturing process. This goal can be achieved by incorporating Design for Manufacturing (DFM) principles specific to the FFF and multi-material (MM) parts. As proof of concept, the design principles were validated for TPU/PLA 3D printed SMPs.

2. Methods and Materials

The quality of a resulting product is influenced by multiple factors, such as the manufacturing process specifics, the operator's experience, the materials, the design, or a combination of those [28], and possibly others. This way, it is essential to understand the correlation between FFF specifics and materials' proprieties to obtain good quality multi-material or multi-component SMPs.

2.1. Design for Multi-material FFF

Design for manufacturing concept refers to a set of best practice guidelines that must be considered to produce a good quality product [29, 30]. Regarding the MM SMPs, the DFM must address FFF and MM printing specifics.

Starting with the printing materials, not all combinations of polymers are possible due to their poor (e.g., ABS/PETG [27]) or lack of affinity (e.g., ABS/PA [27]). In other words, when combined, the resulting MM part is characterised by poor structural integrity. However, using some design principles for single material FFF printers in the design process of MM parts makes obtaining MM parts of dissimilar polymers possible.

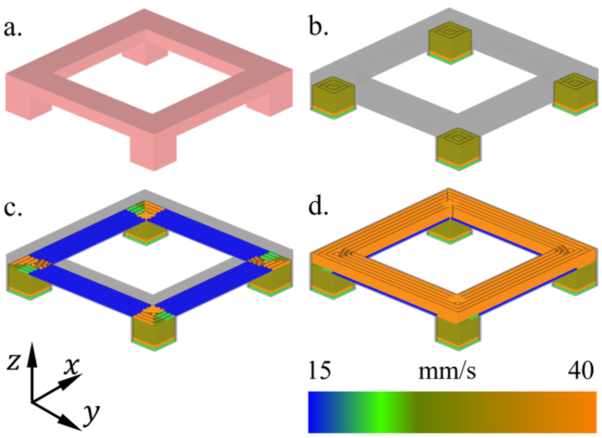

Figure 1: The working principle of bridging for FFF: a. CAD model for suspended printing; b. printed pillars; c. printing of the first suspended layer at a slower speed of 15 mm/s; d. completed part.

Bridging: In FFF, bringing refers to printing without support structures. This can be achieved by creating anchoring points (or pillars) in the deposition path of the extruded materials [31] (Fig. 1.a, b). Yet, this must be assisted by the slow printing speed of the first suspended layer (Fig. 1. c) and proper cooling of the extruded filament to prevent material sagging. After this step, the rest of the part can be printed with higher deposition speeds.

The distance between the anchoring points, printing speed, and cooling depends on the polymers used. However, as a rule of thumb, pillars spaced up to 10 mm can be printed with relatively minor issues [32]. Further parametrisation is needed when increasing the pillar spacing. Secondly, the first layer of the "bridge" should be designed as a multiple of the extrusion width (e.g., 0.4 mm, 0.5 mm) to limit the occurrence of gaps between the extruded filaments.

Embedding refers to fixing one of the MM components (Fig. 2. b) in the body mating material (Fig. 2. a). The main idea is to design the part's components and bodies so that the degrees of freedom of one body are restricted relative to the mating component (Fig. 2. c). Secondly, the embedding component acts as a support structure when printing the other part's components. This is important for ensuring the part's structural integrity. On the other hand, when designing an MM part, the previously presented bridging principles must be integrated into the design to print the MM part with low-compatibility polymers. The pillars design can be asymmetric to the xy plane of the MM part or symmetrical, as presented in Fig. 2.

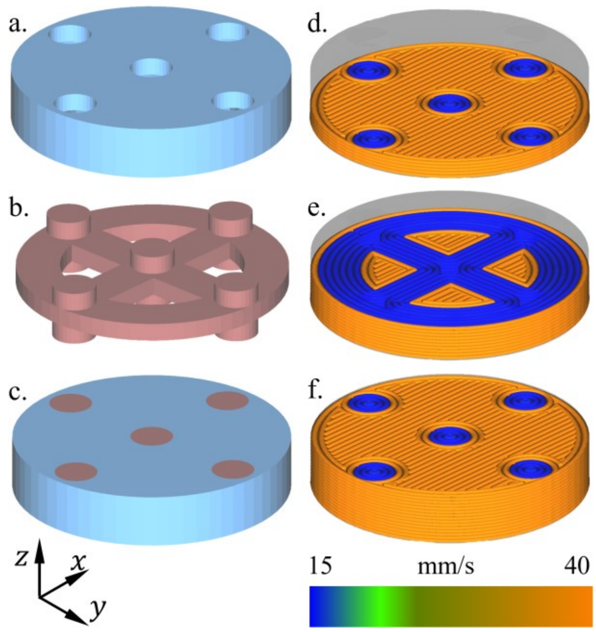

Figure 2: Design principle of an MM part for low-compatibility polymers: a. embedding body; b. embedded body; c. assembled part; d-f. print preview of the part's component at different printing speeds.

After completing the design, the MM parts' bodies are exported as separate entities and reassembled in the printer's slicing tool. Here, a material is assigned to each component, followed by the printing process parametrisation. In this step, the embedding body can be set for regular printing settings (i.e., speed and cooling) and only the embedded body set-up for bridging. The diagram in Fig. 3. d-f highlights how the embedded component is printed only with perimeters at a lower printing speed (e.g., 15 mm/s), referred to as the embedding body.

To summarise the above-presented design considerations, three principal directions must be respected to obtain qualitative MM SMPs (Fig. 3). Those principles are:

- ensure contact on the build plate for all incorporated materials;
- create enough anchoring points for the printed components by considering they are printed in air;
- adjust the printing parameters of the embedded components as they were printed suspended.

In the end, these principles must be treated integrally as their interaction determines how the integrated materials influence the MM design and FFF process parametrisation.

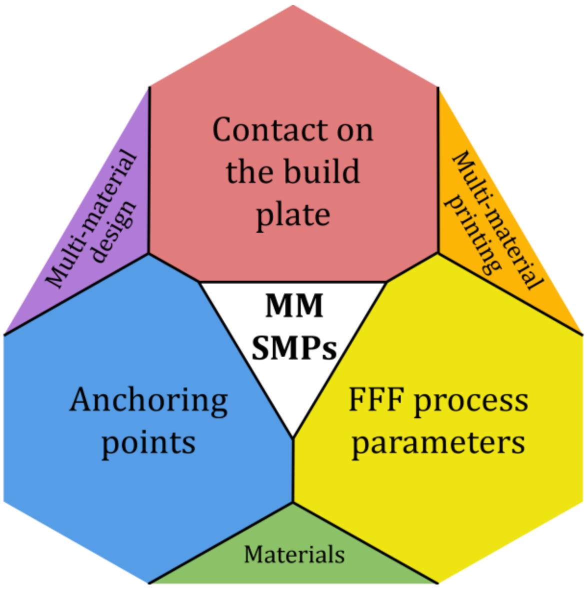

Figure 3: The diagram of design principles for the multi-material SMPs through FFF 3D printing.

The example highlighted in Fig. 2 was realised for two material components and one step of bridging on the vertical. Still, it can be extrapolated for multiple materials components and more complex SMP designs.

2.2. SMS Design

As a proof of concept for the above-presented concepts, an experimental design was created for TPU/PLA SMP in which the PLA is used to "remember" the permanent shape (i.e., results after printing), and TPU is used as an embedding structure. The PLA component was designed based on two spaced beams having 0.8x48.8 mm area with 0.2 mm thickness and seven anchor points spaced by 8 mm. Afterwards, the resulting structure was copied and placed at 8 mm, referring to the previous using a pattern function. A preview of the resulting design is presented in Fig. 4.

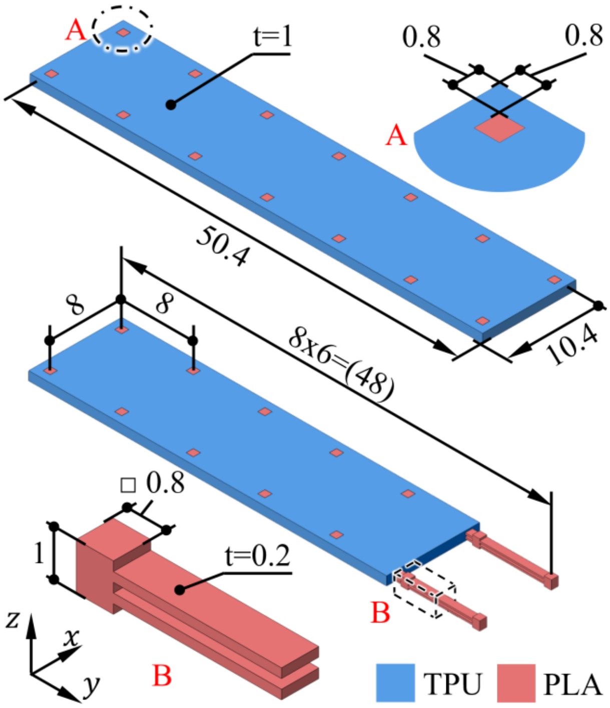

Figure 4: The design structure of the dual-component TPU/PLA SMP. All dimensions are in mm.

The literature review shows that multiple studies investigated the shape memory behaviour of TPU/PLA blends mixed in various ratios (i.e., 50:50, 30:70, 90:10) [33-35]. On the one hand, increasing the TPU ratio improves the overall shape recovery properties. On the other hand, increasing the PLA ratio promotes the shape fixity [18, 33-35]. Distinct from the regular TPU/PLA blend SMP, the one resulting from 3d printing keeps the two polymeric phases macroscopically separate. This way, the PLA ratio was gradually increased to see if the two polymers' ratios influence the shape memory properties similarly.

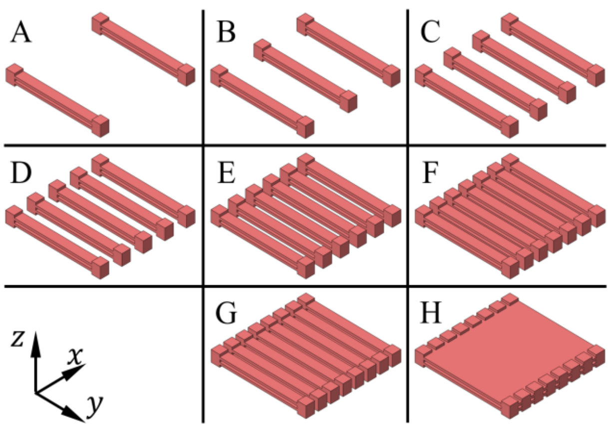

Figure 5: The arrangement of the PLA components in the TPU body of the SMP.

Using the pattern function, the SMP design was modified to increase the number of PLA components up to eight in the 8 mm length. Additionally, in the last design with eight components, the PLA structures were merged in the suspended area. A preview of the arrangement of the PLA components in embedding TPU is presented in Fig. 5.

2.3. SMS Printing

The chosen filaments for the SMPs are commercially available. Those are a black colour Ultrafuse PLA from BASF and a white colour TPU from NinjaFlex. The resulting SMPs were printed using an Ultimaker 3 3D printer in dual extrusion mode using the settings presented in Table 1.

Table 1. Title of the table used for exemplification

1	Nozzle diameter (mm)	0.4
2	Layer height (mm)	0.2
3	Extrusion width (mm)	0.4
4	Walls line count (no.)	0
5	Seam alignment	Back right
6	Top layers (no.)	3
7	Bottom layers (no.)	3
8	Top/Bottom layers pattern	Lines
9	Top/Bottom lines direction (°)	(0;0)/**(90;90)**
10	Extrusion temperature (°C)	215/**240**
11	Build plate temperature(°C)	60
12	Material flow (%)	100/**105**
13	Printing speed (mm/s)	30/**10**
14	First layer speed (mm/s)	20/**10**
15	Retraction distance (mm)	7/**4**
16	Retraction speed (mm/s)	30/**40**
17	Fan speed (%)	100/**25**
18	Maximum fan speed (%)	100/**50**
Values in Bold are associated with the TPU.		

All eight configurations of the SMPs were printed in the same build process without walls and only with solid fill. The TPU component was printed with filaments having a 90° orientation, referred to as the Oy axis, as the PLA with filaments parallel to the same axis (Fig. 6).

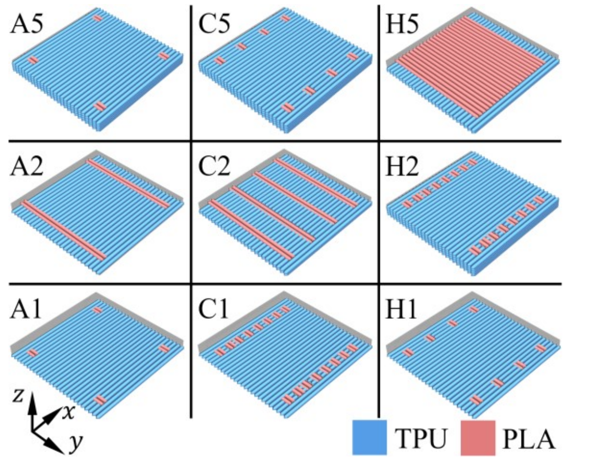

Figure 6: Preview of the print process of the A, C and H SMPs design (according to Fig. 5), where 1, 2 and 5 represent the layer number.

2.4. Testing Methods

The first step consisted of determining the glass transition temperature (Tg) of the PLA filament through Dynamic Mechanical Analysis (DMA) using TA instruments DMA 2980 equipment.

The second step consisted of heating and deforming the SMPs at a temperature of 20°C higher than the PLA's Tg in water, which was constantly measured using a Voltcraft DL-240 thermometer with a TP-208 immersion probe. Then, the temporary shape was obtained by cooling the SMPs in a deformed state at room temperature.

In the third step, the SMPs were reheated at the same temperature. The shape recovery and speed were analysed frame by frame using a digital camera.

3. Results

3.1. DMA Results

A DMA of the PLA filament was done to determine the deformation and recovery temperature of the SMPs based on the resulting Tg. Even if Technical Data Sheets (TDS) are providing Tg as a singular value (i.e., 61°C for PLA and -35°C for TPU). In reality, the glass transition temperature occurs in a range of temperatures [36-38]. The analysis was performed using the multi-frequency method using a single cantilever bending at a frequency of 1 Hz. The temperature scans were made at 2°C/min from 0 to 160°C. Based on the storage modulus, the Tg starts at 57.17°C. It is the temperature at which this PLA blend starts to lose its mechanical properties. According to the loss modulus, the Tg is 63.97°C. According to the tan δ modulus, the upper limit of the Tg range is 68.27°C. All three diagrams are presented in Figure 7. As the SMPs are deformed and reshaped at a temperature 5-20°C higher than the Tg [1, 16, 18], a heat treatment temperature of 80°C was considered optimum for sample shape recovery.

Using a deformation temperature higher than the Tg is important to reduce the spring-back effect and, thus, to improve the fixity ratio of the SMP [39].

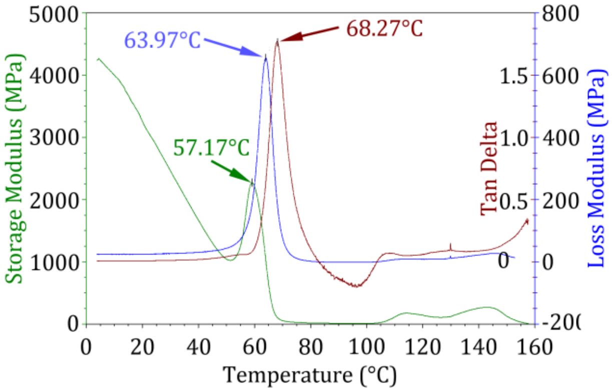

Figure 7: DMA of the chosen PLA filament.

3.2. SMP Evaluation

By analysing the print results, it can be observed that the above-presented design principles can be used in manufacturing the SMPs. Fig. 8 shows that the bridge design enables the PLA component to be printed over the TPU. However, some minor defects can be observed in the structure of the resulting SMPs. Gaps occurred between the TPU extruded filaments, starting with the D sample. This issue can be fixed by increasing the overlap between filaments. Then, going to the PLA body, residues of the black PLA can be observed in the horizontal direction between the anchoring points (C & D samples of Fig. 8). These issues can be solved by adjusting the filament's retraction setting and extrusion temperature (Table 1).

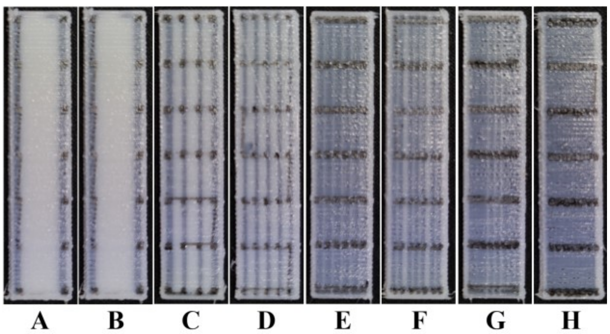

Figure 8: Top view of the resulting 3D printed SMPs.

All SMP samples were submerged in warm water heated at a temperature of 80±2°C. After 5 seconds of heating, each sample was bent at 0° and cooled at room temperature for 20 seconds. As presented in Fig. 9 and 10 in the 0s frames, the samples' shape fixity increases proportionally with the PLA content, with sample H showing the highest degree of fixity.

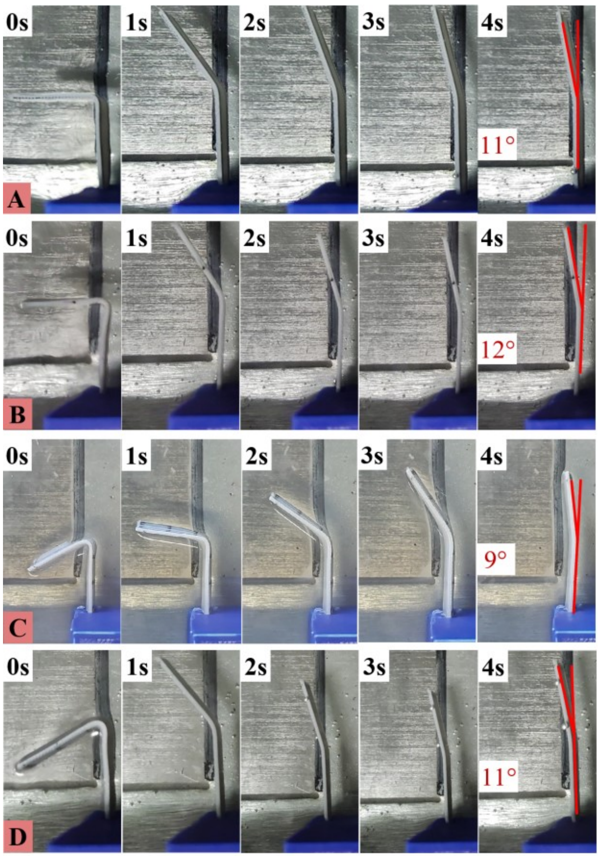

Figure 9: Shape recovery behaviour of the A-D (according to Fig. 5) SMPs during 4s of heating.

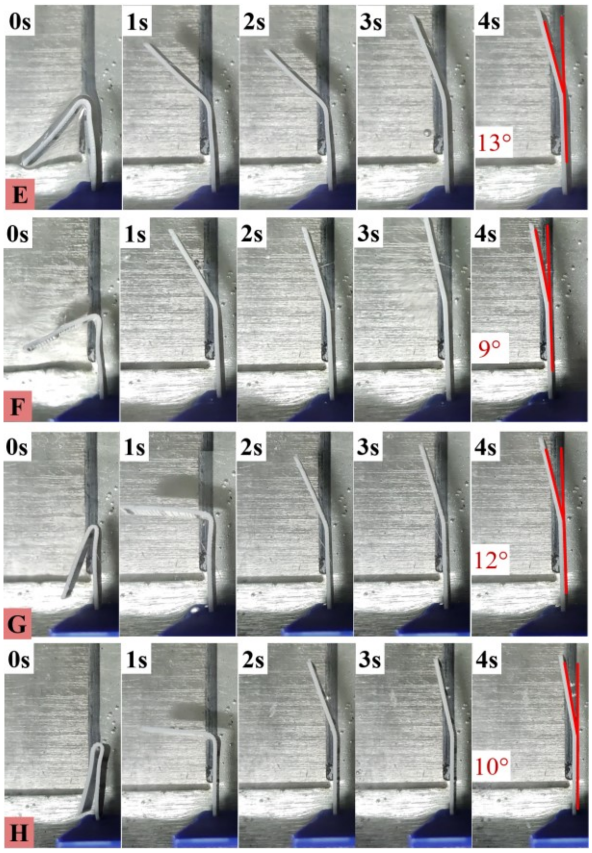

Figure 10: Shape recovery behaviour of the E-H (according to Fig. 5) SMPs during 4s of heating.

After cooling, the SMPs were immersed in water, and the shape recovery behaviour was monitored frame by frame. Overall, the most significant shape change of the samples can be observed in the 1-2s window. In the 3-4s time frame, shape recovery is still going, but to a lower extent than the first time interval.

From the analysed results, it can be observed that none of the analysed SMPs fully recovered their 3D-printed shape. Referring to the initial flat shape (i.e. 180°), the shape recovered samples present a 9-13° bend to the initial shape. From these, C and F showed the best results with a 9° bend to the initial shape.

4. Conclusions

Multi-material FFF technology offers many possibilities regarding the manufacturing of SMPs. However, due to the low affinity of some polymers, most of the available materials cannot be integrated into the same component. To solve some of these limitations, the research of this paper proposed a geometrical way of combining distinct materials by respecting a set of designs for manufacturing principles specific to FFF and multi-material printing.

The main idea is to design the parts components as they were printed in air, without any support structure and only with some anchoring points, similar to a bridge design. Then, all material components must have contact points on the build plate. In the end, the FFF printing process must be parametrised as the parts are printed suspended concerning the polymers' specifics.

The design principles have undergone a validation step, in which eight SMP designs were done accordingly. Furthermore, the resulting designs were tested for shape recovery during heat exposure. The results show that presented design principles can successfully produce SMPs with relatively good shape recovery properties.

Further research must be done to refine the design guild lines of the multi-material SMPs. Those must address the design changes needed based on the polymer processability specifics.

References

[1] Mitchell, A., Lafont, U., Hołyńska, M., & Semprimoschnig, C. (2018) Additive manufacturing-a review of 4D printing and future applications, Addit. Manuf., Vol. 24, Pp. 606–626. https://doi.org/10.1016/j.addma.2018.10.038

[2] Scalet, G. (2020). Two-way and multiple-way shape memory polymers for soft robotics: An overview. Actuators, Vol. 9, Issue 1 Pp. 10. https://doi.org/10.3390/act9010010

[3] Valvez, S., Reis, P. N., Susmel, L., & Berto, F. (2021). Fused filament fabrication-4D-printed shape memory polymers: a review. Polymers, Vol. 13, Issue 5, Pp. 701. https://doi.org/10.3390/polym13050701

[4] Ameen, A. A., Takhakh, A. M., & Abdal-hay, A. (2023). An Overview of the Latest Research on the Impact of 3D Printing Parameters on Shape Memory Polymers. Eur. Polym. J., Vol. 194, Pp. 112145. https://doi.org/10.1016/j.eurpolymj.2023.112145

[5] Leist, S. K., Gao, D., Chiou, R., & Zhou, J. (2017). Investigating the shape memory properties of 4D printed polylactic acid (PLA) and the concept of 4D printing onto nylon fabrics for the creation of smart textiles. Virtual Phys. Prototyp., Vol. 12, Issue 4, Pp. 290-300. https://doi.org/10.1080/17452759.2017.1341815

[6] Goo, B., Hong, C. H., & Park, K. (2020). 4D printing using anisotropic thermal deformation of 3D-printed thermoplastic parts. Materials & Design, Vol. 188, Pp. 108485. https://doi.org/10.1016/j.matdes.2020.108485

[7] Rafiee, M., Farahani, R. D., & Therriault, D. (2020). Multi-material 3D and 4D printing: a survey. Advanced Science, Vol 7 Issue 12, Pp. 1902307. https://doi.org/10.1002/advs.201902307

[8] Kafle, A., Luis, E., Silwal, R., Pan, H. M., Shrestha, P. L., & Bastola, A. K. (2021). 3D/4D Printing of polymers: Fused deposition modelling (FDM), selective laser sintering (SLS), and stereolithography (SLA). Polymers, Vol. 13 Issue 18, Pp. 3101. https://doi.org/10.3390/polym13183101

[9] Mustapha, K. B., & Metwalli, K. M. (2021). A review of fused deposition modelling for 3D printing of smart polymeric materials and composites. Eur. Polym. J., Vol.156, Pp. 110591. https://doi.org/10.1016/j.eurpolymj.2021.110591

[10] Suhail, R., Chen, J. F., Amato, G., & McCrum, D. (2020). Mechanical behaviour of NiTiNb shape memory alloy wires–strain localisation and effect of strain rate. Mechanics of Materials, Vol.144, Pp. 103346. https://doi.org/10.1016/j.mechmat.2020.103346

[11] Kumar, S. S., Arohi, A. C., & Sen, I. (2022). A Review on Micro-mechanical Testing of NiTi-Based Shape Memory Alloys. J. of the Indian Institute of Sci., Vol. 102, Issue 1, Pp. 211-235. https://doi.org/10.1007/s41745-021-00278-6

[12] Carlson, M., & Li, Y. (2020). Development and kinetic evaluation of a low-cost temperature-sensitive shape memory polymer for 4-dimensional printing. The International Journal of Advanced Manufacturing Technology, Vol. 106, Pp. 4263-4279. https://doi.org/10.1007/s00170-020-04927-5

[13] Sorimpuk, N. P., Choong, W. H., & Chua, B. L. (2022). Thermoforming characteristics of PLA/TPU multi-material specimens fabricated with fused deposition modelling under different

temperatures. Polymers, Vol. 14, Issue 20, Pp. 4304. https://doi.org/10.3390/polym14204304

[14] ERMOLAI, V., SOVER, A., NAGÎȚ, G., & IRIMIA, A. I. (2023). Shape recovery properties of PET-based 3D printed samples. Acta Technica Napocensis-Series: Applied Mathematics, Mechanics, and Engineering, Vol., 65, Issue 4S.

[15] Liu, T., Liu, L., Zeng, C., Liu, Y., & Leng, J. (2020). 4D printed anisotropic structures with tailored mechanical behaviors and shape memory effects. Composites Science and Technology, Vol. 186, Pp. 107935. https://doi.org/10.1016/j.compscitech.2019.107935

[16] Khalid, M. Y., Arif, Z. U., Noroozi, R., Zolfagharian, A., & Bodaghi, M. (2022). 4D printing of shape memory polymer composites: A review on fabrication techniques, applications, and future perspectives. Journal of Manufacturing Processes, Vol. 81, Pp. 759-797. https://doi.org/10.1016/j.jmapro.2022.07.035

[17] Ding, Q., Chen, J., Yan, W., Yan, K., Kyme, A., & Cheng, S. S. (2022). A high-performance modular SMA actuator with fast heating and active cooling for medical robotics. IEEE/ASME Transactions on Mechatronics, Vol. 27, Issue 6, Pp. 5902-5913. https://doi.org/10.1109/TMECH.2022.3190930

[18] Razzaq, M. Y., Gonzalez-Gutierrez, J., Mertz, G., Ruch, D., Schmidt, D. F., & Westermann, S. (2022). 4D printing of multicomponent shape-memory polymer formulations. Applied Sciences, Vol. 12, Issue 15, Pp. 7880. https://doi.org/10.3390/app12157880

[19] Costa, D. C., Costa, P. D., Gomes, M. C., Chandrakar, A., Wieringa, P. A., Moroni, L., & Mano, J. F. (2022). Universal strategy for designing shape memory hydrogels. ACS Materials Letters, Vol. 4, Issue 4, Pp. 701-706. https://doi.org/10.1021/acsmaterialslett.2c00107

[20] Hosseini, S., Farrokhabadi, A., & Chronopoulos, D. (2023). Experimental and numerical analysis of shape memory sinusoidal lattice structure: Optimization through fusing an artificial neural network to a genetic algorithm. Composite Structures, Vol. 323, Pp. 117454. https://doi.org/10.1016/j.compstruct.2023.117454

[21] Martin, K. A., Thornell, T. L., Hanna, H. A., Weiss, C. A., & McClelland, Z. B. (2024). Effect of Filament Color and Fused Deposition Modeling/Fused Filament Fabrication Process on the Development of Bistability in Switchable Bistable Squares. ASME Open J. of Engineering, Vol.3., Pp. 031002. https://doi.org/10.1115/1.4064142

[22] Sharma, A., & Singholi, A. K. S. (2021). Shape memory and mechanical characterization of polylactic acid wood composite fabricated by fused filament fabrication 4D printing technology. Materialwissenschaft und Werkstofftechnik, Vol. 52, Issue 6, Pp. 635-643. https://doi.org/10.1002/mawe.202000284

[23] Carrell, J., Gruss, G., & Gomez, E. (2020). Four-dimensional printing using fused-deposition modeling: a review. R. Prototyp. J., Vol. 26, Issue 5, Pp. 855-869. https://doi.org/10.1108/RPJ-12-2018-0305

[24] Ermolai, V., Sover, A., & Lang, A. Characterisation of the shape memory effect of PET polymer by FFF 3D printing. Materials Research Proceedings, Vol. 28, Pp. 93-100. https://doi.org/10.21741/9781644902479-11

[25] Sharma, A., & Rai, A. (2022). Fused deposition modelling (FDM) based 3D & 4D Printing: A state of art review. Materials Today: Proceedings, Vol. 62, Pp. 367-372. https://doi.org/10.1016/j.matpr.2022.03.679

[26] Nazir, A., Gokcekaya, O., Billah, K. M. M., Ertugrul, O., Jiang, J., Sun, J., & Hussain, S. (2023). Multi-material additive manufacturing: A systematic review of design, properties, applications, challenges, and 3D Printing of materials and cellular metamaterials. Materials & Design, Vol. 226, Pp. 111661. https://doi.org/10.1016/j.matdes.2023.111661

[27] Mihalache, A. M., Ermolai, V., Sover, A., Nagîț, G., Boca, M. A., Slătineanu, L., ... & Rîpanu, M. I. (2022). Tensile Behavior of Joints of Strip Ends Made of Polymeric Materials. Polymers, Vol. 14, Issue 22, Pp. 4990. https://doi.org/10.3390/polym14224990

[28] Ermolai, V., Sover, A. (2023). Multi-material 3D Printed Interfaces. Influencing Factors and Design Considerations. In: Cioboată, D.D. (eds) International Conference on Reliable Systems Engineering (ICoRSE) - 2023. ICoRSE 2023. Lecture Notes in Networks and Systems, vol 762. Springer, Cham. https://doi.org/10.1007/978-3-031-40628-7_11

[29] Formentini, G., Boix Rodríguez, N., & Favi, C. (2022). Design for manufacturing and assembly methods in the product development process of mechanical products: a systematic literature review. The International J. of Advanced Manufacturing Technology, 120(7-8), Pp. 4307-4334. https://doi.org/10.1007/s00170-022-08837-6

[30] Vaneker, T., Bernard, A., Moroni, G., Gibson, I., & Zhang, Y. (2020). Design for additive manufacturing: Framework and methodology. CIRP Annals, Vol. 69, Issue 2, Pp. 578-599. https://doi.org/10.1016/j.cirp.2020.05.006

[31] Ghorbani, J., Koirala, P., Shen, Y. L., & Tehrani, M. (2022). Eliminating voids and reducing mechanical anisotropy in fused filament fabrication parts by adjusting the filament extrusion rate. Journal of Manufacturing Processes, Vol. 80, Pp. 651-658. https://doi.org/10.1016/j.jmapro.2022.06.026

[32] Patterson, A. E., Chadha, C., & Jasiuk, I. M. (2021). Identification and mapping of manufacturability constraints for extrusion-

based additive manufacturing. J. of Manufacturing and Materials Processing, Vol. 5, Issue 2, Pp. 33. https://doi.org/10.3390/jmmp5020033

[33] Lai, S. M., & Lan, Y. C. (2013). Shape memory properties of melt-blended polylactic acid (PLA)/thermoplastic polyurethane (TPU) bio-based blends. J. of Polymer Research, Vol. 20, Issue 5. https://doi.org/10.1007/s10965-013-0140-6

[34] Shin, E. J., Jung, Y. S., Park, C. H., & Lee, S. (2023). Eco-friendly TPU/PLA Blends for Application as Shape-Memory 3D Printing Filaments. J. of Polymers and the Environment, Vol. 31, Pp. 3182–3196. https://doi.org/10.1007/s10924-023-02799-w

[35] Song, J. J., Srivastava, I., Kowalski, J., & Naguib, H. E. Fabrication and characterization of a foamed polylactic acid (PLA)/thermoplastic polyurethane (TPU) shape memory polymer (SMP) blend for biomedical and clinical applications. In Behavior and Mechanics of Multifunctional Materials and Composites 2014, Vol. 9058, Pp. 86-98. SPIE. https://doi.org/10.1117/12.2046494

[36] Quiñonez PA, Ugarte-Sanchez L, Bermudez D, Chinolla P, Dueck R, Cavender-Word TJ, Roberson DA. (2021) Design of Shape Memory Thermoplastic Material Systems for FDM-Type Additive Manufacturing. Materials, Vol. 14, Issue 15, Pp. 4254. https://doi.org/10.3390/ma14154254

[37] Yi, S., Oh, N., Min, K. E., Shin, J. S., & Kim, C. (2023). Thermo-Viscoelastic Characterization of 3D Printing Polymers. Applied Sciences, Vol. 13, Issue 5, Pp. 2876. https://doi.org/10.3390/app13052876

[38] Caputo, P., Calandra, P., Pecchia, A., Tirri, B., Mercuri, F., Celso, F. L., ... & Rossi, C. O. (2024). Reinforcement of Polylactic Acid/Poly Butylene Adipate-co-Terephthalate blends by starch addition: A coupled computational and experimental study. Colloids and Surfaces A: Physicochemical and Engineering Aspects, vol. 685, Pp. 133159. https://doi.org/10.1016/j.colsurfa.2024.133159

[39] Li, G., & Wang, A. (2016). Cold, warm, and hot programming of shape memory polymers. Journal of Polymer Science Part B: Polymer Physics, Vol. 54, Issue 14, Pp. 1319-1339. https://doi.org/10.1002/polb.24041